Published OnlineFirst September 24, 2014; DOI: 10.1158/2326-6066.CIR-14-0154

Cancer Immunology Miniatures

Cancer Immunology Research

Immune Activation and a 9-Year Ongoing Complete Remission Following CD40 Antibody Therapy and Metastasectomy in a Patient with Metastatic Melanoma

David L. Bajor[1,2,3], Xiaowei Xu[1,4], Drew A. Torigian[1,5], Rosemarie Mick[1,6], Laura R. Garcia[2], Lee P. Richman[2], Cindy Desmarais[7], Katherine L. Nathanson[1,3], Lynn M. Schuchter[1,2,3], Michael Kalos[1,4], and Robert H. Vonderheide[1,2,3]

Abstract

Direct immune activation via agonistic mAbs is a potentially complementary approach to therapeutic blockade of inhibitory immune receptors in cancer. Here, we provide genetic analysis of the immunologic consequences associated with the use of an agonistic CD40 mAb in a patient with metastatic melanoma who responded, underwent a single metastasectomy, and then achieved a complete remission ongoing for more than 9 years after starting therapy. Tumor microenvironment after immunotherapy was associated with proinflammatory modulations and emergence of a *de novo* T-cell repertoire as detected by next-generation sequencing of T-cell receptors (TCR) in the tumor and blood. The *de novo* T-cell repertoire identified in the posttreatment metastasectomy sample was also present—and in some cases expanded—in the circulation years after completion of therapy. Comprehensive study of this "exceptional responder" highlights the emerging potential of direct immune agonists in the next wave of cancer immunotherapies and a potential role for TCR deep sequencing in cancer immune assessment. *Cancer Immunol Res; 2(11); 1051–8. ©2014 AACR.*

Introduction

The cell-surface molecule CD40 is a member of the tumor necrosis factor receptor (TNFR) superfamily and is a critical mediator of immune activation (1). Ligation of CD40 on antigen-presenting cells (APC) mediates direct immune activation, including upregulation of costimulatory molecules and other immune mediators (2). Clinically, germline mutations in CD40 or its receptor CD40 ligand, which is expressed primarily by activated T lymphocytes, result in major immune deficiencies (3). Landmark studies in murine systems demonstrated that agonistic CD40 mAbs can fully substitute for T-cell help *in vivo* (4–6) and trigger T-cell–mediated immune rejection of tumors (7–9). CD40 agonistic agents therefore have been developed as potential therapy for cancer, with promising results in early studies (2). CP-870,893, a fully human IgG2 mAb (Pfizer/Roche), is the most potent CD40 agonist (10), does not require Fc receptor crosslinking (11), and in multiple phase I studies has been evaluated for safety and optimal dose and schedule (12–16). Although systemic immune activation and objective tumor responses have been described in patients receiving CP-870,893 (12), its impact on T-cell activation in the tumor microenvironment and its potential for inducing durable complete remission have not been described.

Patients, Materials, and Methods

Clinical trial

The patient was enrolled in an Institutional Review Board (IRB)–approved, phase I clinical trial at the Abramson Cancer Center (NCT02225002) and received a single intravenous dose (0.2 mg/kg, the maximum tolerated dose) of CP-870,893 (Pfizer/Roche), and was found 4 weeks later to have a partial tumor response (12). The patient then received nine additional doses of CP-870,893 (0.2 mg/kg per dose every 6–14 weeks) on an investigator-sponsored, IRB-approved clinical trial for patients for whom a single dose was associated with tumor response without limiting toxicity from CP-870,893 (NCT02157831). The dosing intervals varied because the protocol initially required demonstration, after each cycle, of the absence of human anti-human antibodies (HAHA) to CP-870,893. This requirement was eliminated when no HAHAs were detected in the first 29 patients of the parent protocol (NCT02225002). Toxicity grades were based on the NCI Common Toxicity Criteria Version 3.0 (Supplementary Table S1);

[1]Abramson Cancer Center, University of Pennsylvania, Philadelphia. [2]Abramson Family Cancer Research Institute, University of Pennsylvania, Philadelphia. [3]Department of Medicine, Perelman School of Medicine, University of Pennsylvania, Philadelphia. [4]Department of Pathology, Perelman School of Medicine, University of Pennsylvania, Philadelphia. [5]Department of Radiology, Perelman School of Medicine, University of Pennsylvania, Philadelphia. [6]Department of Biostatistics and Epidemiology, Perelman School of Medicine, University of Pennsylvania, Philadelphia. [7]Adaptive Biotechnologies, Seattle, Washington.

Note: Supplementary data for this article are available at Cancer Immunology Research Online (http://cancerimmunolres.aacrjournals.org/).

Corresponding Author: Robert H. Vonderheide, University of Pennsylvania School of Medicine, 8-121 SCTR, 3400 Civic Center Boulevard, Philadelphia, PA 19104. Phone: 215-573-4265; Fax: 215-573-2652; E-mail: rhv@exchange.upenn.edu

doi: 10.1158/2326-6066.CIR-14-0154

Published OnlineFirst September 24, 2014; DOI: 10.1158/2326-6066.CIR-14-0154

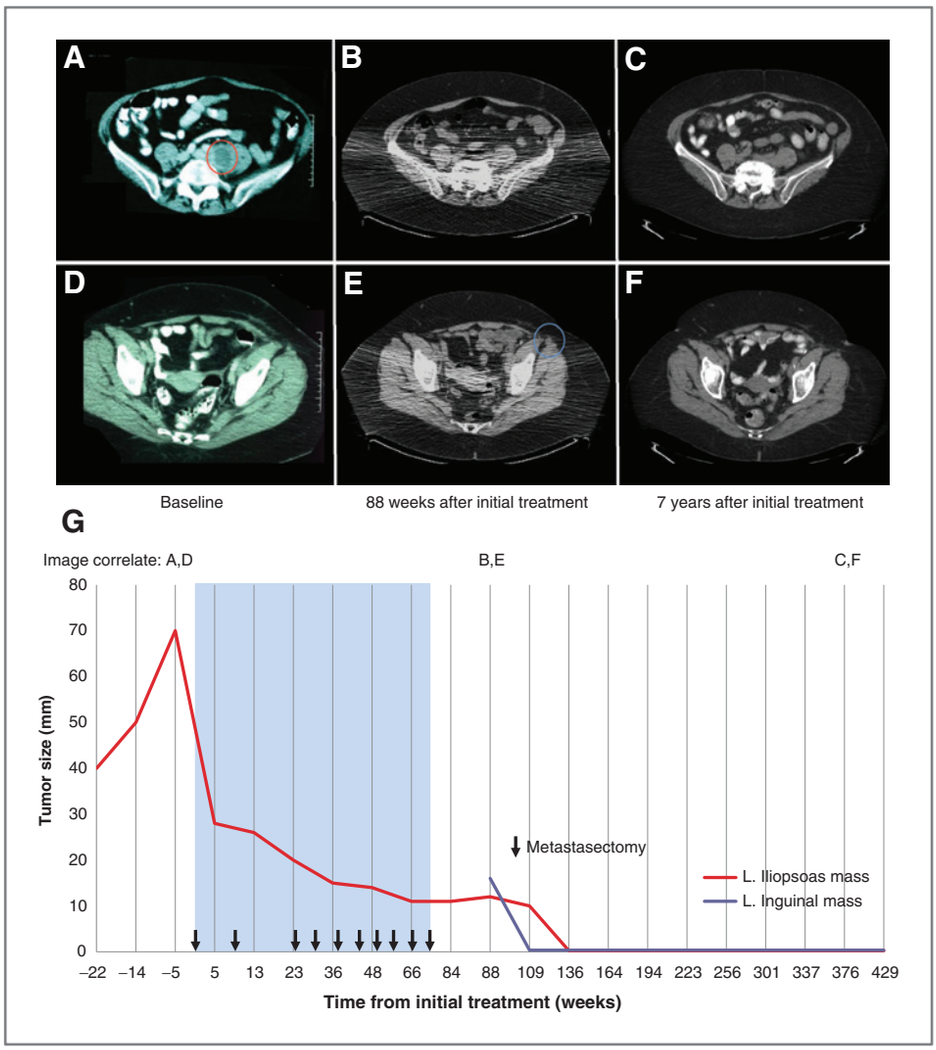

Figure 1. Imaging response following treatment with CP-870,893. A–F, serial axial CT images of two anatomical regions with tumor involvement. A and D, baseline images; B and E, after 10 infusions of CP-870,893; C and F, after an additional 5 years of clinical follow-up. Images correspond to the timeline in G, as indicated. Red circle indicates a left iliopsoas mass and blue circle indicates a lesion detected in the left anterior thigh that had FDG uptake (not shown) and that was resected after CP-870,893 treatment. G, size of the patient's melanoma lesions over the 9-year course of treatment with CP-870,893, metastasectomy, and clinical observation (arrows within blue panel indicate CP-870,893 infusions).

objective tumor responses were based on RECIST assessment of serial CT scans. The patient also underwent serial chest, abdomen, and pelvis 2[18F]fluoro-2-deoxy-D-glucose (FDG) positron emission tomography/computed tomography ([^{18}F]-FDG-PET/CT) examinations.

Histopathology

Immunohistochemical staining was performed on 5-μm-thick, formalin-fixed, paraffin-embedded (FFPE) sections of resected metastatic tumor. Tumor samples included involved inguinal lymph nodes (before CP-870,893 treatment) and a resected thigh mass (after treatment with CP-870,893). Heat-induced epitope retrieval was performed as previously described (17). Slides were incubated with a primary antibody for 1 hour at room temperature. Staining was done on a DakoCytomation Autostainer using the EnVision+ horseradish peroxidase (HRP) DAB system (DakoCytomation) according to the manufacturer's recommendations. Normal mouse serum (1:1,000 dilution) was substituted for the primary antibody in each case as a negative control. Images were taken using a LEICA DFC420 mounted on a Leica DMLB microscope.

Gene expression analysis

Multiplex gene expression analysis was performed on FFPE-resected tumor samples collected before and after treatment. RNA quantification was performed directly from FFPE lysates without enzymatic amplification using branch DNA signal amplification via the QuantiGene platform (Affymetrix, Inc.) and a custom-designed QuantiGene Plex 2.0 assay panel, following the manufacturer instructions. Data were acquired on a FlexMAP-3D instrument and analyzed using xPONENT software v4.0. Each sample was evaluated in a 3-fold dilution series, with sample values within the linear range and above the statistical mean of the background value used to quantify transcript abundance. To enable intersample comparison, dilution-adjusted mean fluorescence intensity values were normalized for total input mRNA using the housekeeping gene PP1B. For each transcript detection, integrity was determined using mRNA obtained from activated lymphocytes and

Published OnlineFirst September 24, 2014; DOI: 10.1158/2326-6066.CIR-14-0154

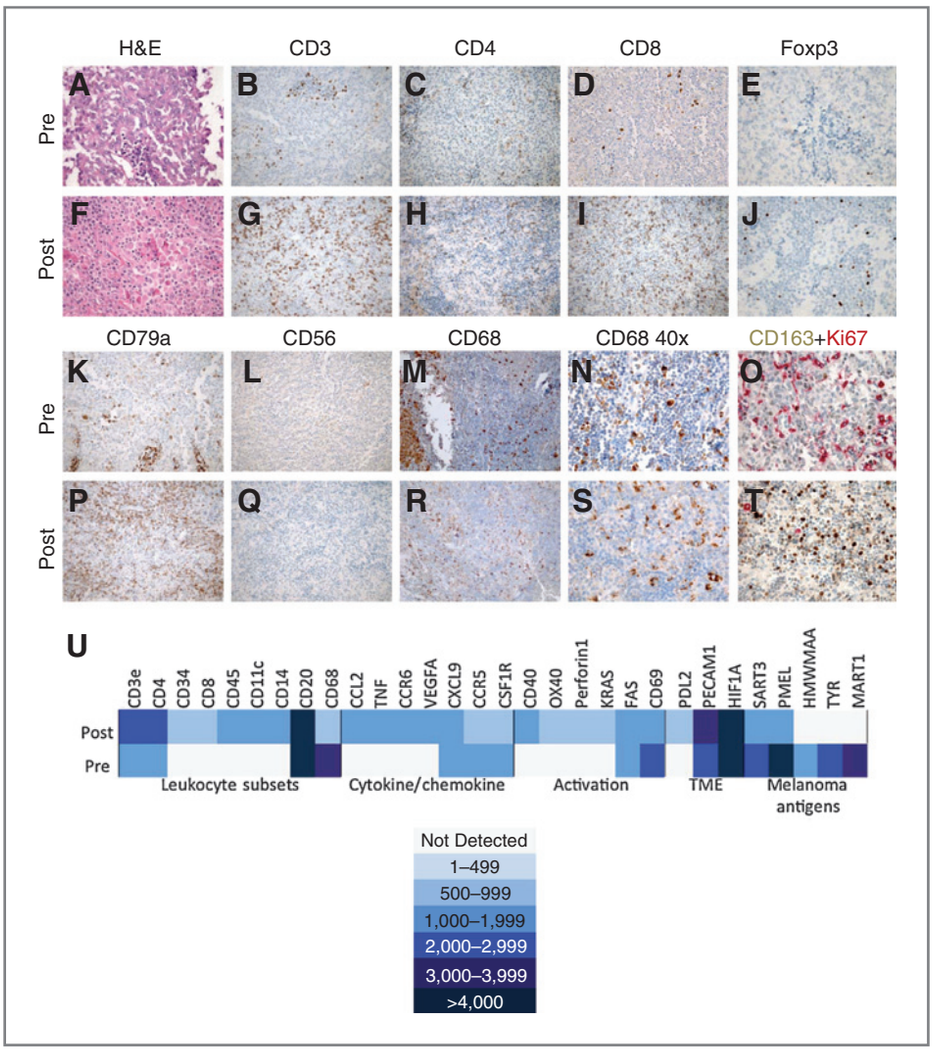

Figure 2. Changes in the tumor microenvironment after treatment with CP-870,893. A and F, hematoxylin and eosin (H&E) staining of pretreatment and posttreatment tumor specimens, respectively. B–E and K–O, immunohistochemical analyses of pretreatment specimens; G–J and P–T, corresponding posttreatment specimens. All images are magnified by a factor of 20 unless otherwise noted. U, map shows relative gene expression in the tumor before and following treatment with CP-870,893 for leukocyte subsets, cytokines/chemokines, leukocyte activation markers, microenvironment markers, and melanoma-associated antigens.

melanoma tumor cell lines. Data for detectable transcripts are included in the main text; the remaining data are included in Supplementary Table S2.

Fluorescence-activated cell sorting

Whole blood was collected in green top (heparin sulfate) BD vacutainer tubes (Becton Dickinson), processed to obtain peripheral blood mononuclear cells (PBMC) using Ficoll-Paque PLUS (GE Healthcare), and frozen in 10% DMSO at −150°C. For sorting, PBMCs were thawed, washed, and labeled with CD3-V450, CD8-FITC, CD4-V500, CD127-PE, CD19-PerCP, CD14-PerCP, and CD25-APC antibodies (Becton Dickinson), and T-cell subsets were sorted using a BD Influx (Becton Dickinson). Cytotoxic T cells were defined as $CD3^+$, $CD8^+$, $CD4^-$, $CD14^-$, and $CD19^-$, and T-helper cells were defined as $CD3^+$, $CD4^+$, $CD8^-$, $CD127^+$, $CD25^-$, $CD14^-$, and $CD19^-$.

Deep sequencing of T-cell receptor β chain

High-throughput next-generation sequencing of the T-cell receptor beta (TCRβ) CDR3 region was performed in collaboration with Adaptive Biotechnologies using the ImmunoSEQ platform. Genomic DNA was isolated from paraffin-embedded tumor tissues, from unsorted PBMCs, or from $CD4^+$ or $CD8^+$ T lymphocytes sorted from peripheral blood via an Influx Cell Sorter (BD Biosciences). DNA was subjected to combined multiplex PCR, followed by sequencing and algorithmic analyses to quantify individual TCRβ sequences in samples, as described (18). Reads per unique TCRβ sequence were divided by overall number of TCRβ sequence reads per sample to estimate the frequency of each clone. To focus on the most frequent tumor-infiltrating clones, the "top-quartile (TQ) clones" were identified in each of the tumor samples by ranking the unique clones in each sample in order of frequency until a cumulative total of 25% of all T lymphocytes in each sample was reached. This analytic technique for identifying high-frequency clones was recently described by Cha and colleagues (19).

Results

Case report

A 61-year-old woman with recurrent, metastatic melanoma presented for consideration of a phase I clinical trial of CP-870,893 (NCT02225002). The patient was initially diagnosed

Published OnlineFirst September 24, 2014; DOI: 10.1158/2326-6066.CIR-14-0154

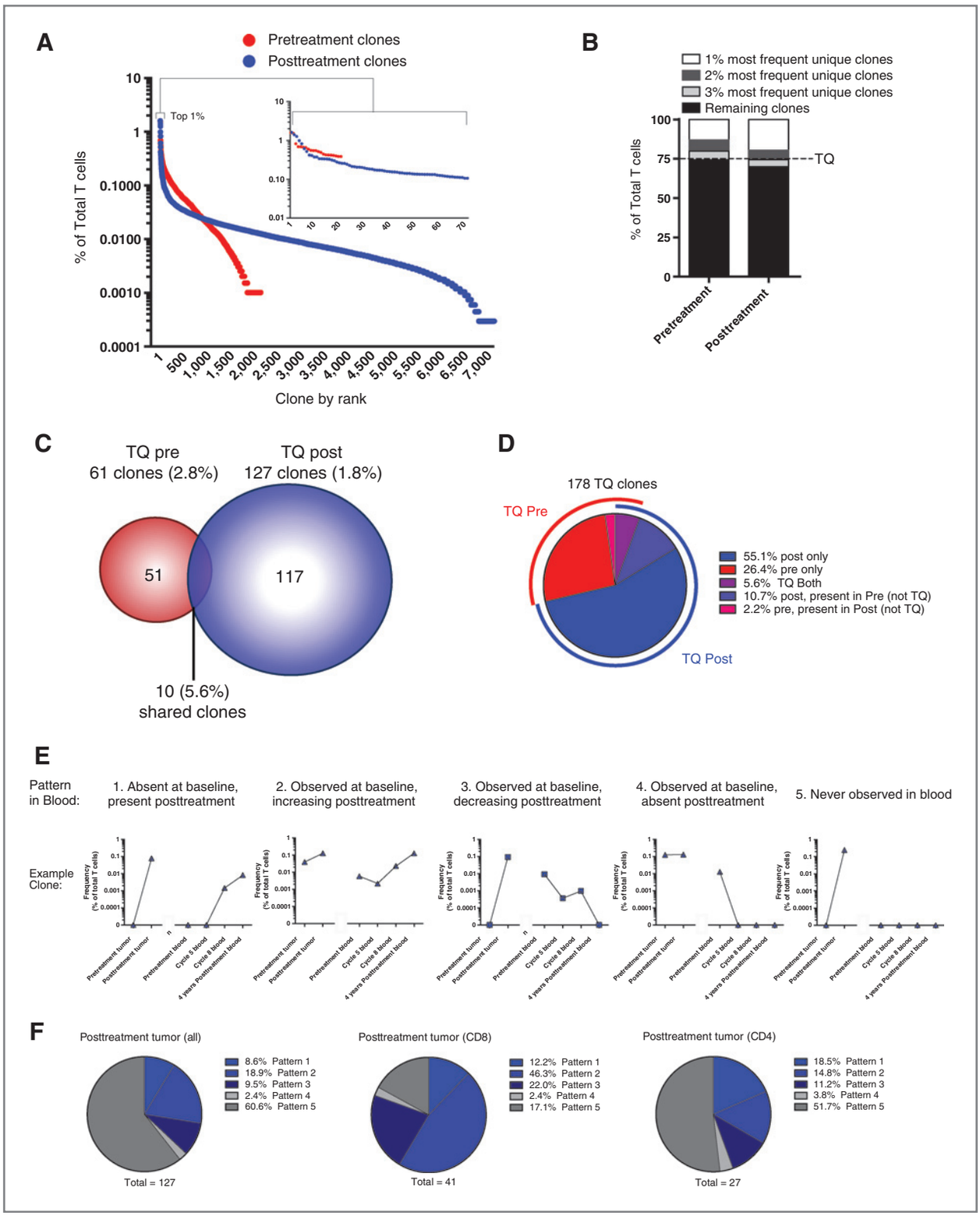

Figure 3. Identification and tracking of tumor-infiltrating lymphocytes by TCRβ deep sequencing. For each unique T-cell clone detected in the pretreatment and posttreatment tumor specimens, A displays the percentage of each clone among total T cells as a function of rank, starting with the most common clones at the left of the axis. Inset shows this pattern for the top 1% of clones in each sample. Each symbol represents a unique clone. B, the top first, second, and third percentage of the most frequent clones as a function of the total percentage of T cells in each sample. (*Legend continued on the following page.*)

Published OnlineFirst September 24, 2014; DOI: 10.1158/2326-6066.CIR-14-0154

with melanoma of the left ankle in 2002 and underwent wide local excision of a 15-mm lesion (depth of 8 mm); sentinel lymph node dissection revealed one inguinal lymph node positive for melanoma. Comprehensive lymph node dissection produced 13 lymph nodes, all negative for melanoma. The patient was treated with high-dose IFNα, but in 2003, developed in-transit metastases on the anterior left thigh and lymphadenopathy in the left groin. The patient underwent surgical excision of two in-transit metastases and further exploration of the groin with additional inguinal lymph node removal (13/19 positive), followed by an isolated limb perfusion with high-dose melphalan. In subsequent analyses, this surgical specimen was used as a pretreatment sample. Relapse of melanoma in the left lower extremity and inguinal region was diagnosed 6 months later. The patient was treated with temozolomide and imatinib on a phase I clinical trial (NCT00667953) with resolution of subcutaneous nodules in the anterior left thigh; however, a focus of disease in the left iliopsoas muscle progressed on consecutive response assessments so the patient was referred for treatment with CP-870,893. At study entry, Eastern Cooperative Oncology Group performance status (ECOG-PS) was 0, and serum laboratory studies indicated normal organ function. CT of the chest, abdomen, and pelvis and [^{18}F]-FDG-PET/CT demonstrated progressive disease in the pelvis involving the left iliopsoas muscle (70-mm mass; Fig. 1A).

The patient enrolled in a phase I clinical trial of a single intravenous infusion of CP-870,893 at 0.2 mg/kg (NCT02225002). Tumor restaging at 4 weeks showed evidence of a partial response (Fig. 1), and the patient then received nine additional infusions of CP-870,893 (0.2 mg/kg) every 6 to 14 weeks over the next 67 weeks on a separate investigator-sponsored clinical trial for patients responding to treatment on the single-dose trial (NCT02157831). Cytokine-release syndrome (grade 1 or 2) occurred with each infusion characterized by transient low-grade fevers, rigor, and myalgias, with rapid symptomatic resolution after treatment with acetaminophen, ibuprofen, and/or meperidine. No grade 3 or 4 adverse events were observed except grade 3 leukopenia, lymphopenia, or neutropenia on some cycles on the day after infusion, returning to grade 1 or lower by day 3 (Supplementary Table S1). Restaging after the sixth dose of CP-870,893 revealed a near-complete response by RECIST criteria and complete resolution of FDG uptake by the iliopsoas mass. After four additional infusions of CP-870,893 and no changes in the lesion by imaging, the patient was presumed to have a complete response and was taken off study and observed. Eight weeks later, an FDG-avid 15-mm mass was appreciated in the left upper thigh (Fig. 1E) that was not visualized at baseline (Fig. 1D) or previously. The lesion was resected and found to be metastatic melanoma. The patient received no further therapy, and has been restaged every 6 to 12 months since 2006 (most recently July 2014). During this observation, the patient's pretreatment tumor was evaluated and found to possess a BRAF V600E mutation (c-kit mutations were not determined). The patient has never received mAbs to CTLA-4, PD-1, or PD-L1, nor B-Raf or MEK inhibitors. By November 2007, there was resolution of the iliopsoas mass with no other evidence of disease (Fig. 1C and F). The patient remains in good health and in complete remission with an ECOG-PS of 0 more than 9 years after initial therapy with CP-870,893. Longitudinally collected tumor and blood biospecimens were analyzed according to methods described above.

Immune assessment of tumor tissues

Immunohistochemical staining of the inguinal lymph node dissection specimen obtained 13 months before treatment revealed scant infiltration of CD3$^+$ T cells and CD79a$^+$ B cells, with most cells found in the perivascular areas (Fig. 2, pre plots). The metastasectomy specimen, taken 19 weeks after cessation of treatment, showed extensive lymphoid infiltration admixed with tumor cells (Fig. 2, post plots). This included a dense CD3$^+$ T-cell infiltrate comprised largely of CD8$^+$ T cells. Infiltration of CD4$^+$ T cells was similar before and after treatment, whereas the number of intratumoral CD4$^+$ Foxp3$^+$ T cells, either regulatory T cells (Treg) or acutely activated effector cells, increased. CD56$^+$ natural killer cells were minimally present in both pretreatment and posttreatment tumors. CD68$^+$ macrophages were present in large numbers in both specimens, and CD163$^+$ cells, representing alternatively activated (often called M2) immunosuppressive macrophages, were increased after treatment. The mechanism by which the number of CD163$^+$ macrophages increased in the posttreatment tumor is not clear and worthy of further study in patients treated with CP-870,893. Prominent Ki-67 staining of actively proliferating tumor cells was observed in the pretreatment tumor sample and was considerably reduced in the posttreatment specimen. Reduced Ki-67 staining likely reflects a reduced number of dividing tumor cells, consistent with the hypothesized antitumor adaptive response.

Quantitative gene expression analyses of the baseline (pretreatment) and metastasectomy (posttreatment) tumor biopsy specimens demonstrated a profile concordant with the histologic and immunohistochemical analyses, and a signature consistent with extensive and broad immune activation (Fig. 2U). For example, in the posttreatment sample, robust increases in transcripts for leukocytes (CD45), T cells (CD3e, CD4, CD8), dendritic cells (CD11c), and macrophages (CD14) were observed along with elevation in transcripts associated with proinflammatory cytokines/chemokines (CCL2, TNF, CCR6) and immune activation and effector functions (CD40, OX40, perforin, KRAS). By normalizing expression of each transcript in each tumor sample to CD3, we found that the increased gene signatures after treatment were not explained

(*Continued*.) TQ clones are the subset of the most frequent unique clones that together comprise 25% of total T cells. C, the number of TQ clones in each sample and the overlaps in the two samples. D indicates as a percentage the distribution of all TQ clones in either pretreatment, posttreatment, or in both samples. E, five patterns of change in blood frequency of TQ clones in the posttreatment sample that can be identified by serially tracking with TCRβ deep sequencing. Five exemplary clones are shown, one for each pattern. F, percentage of TQ posttreatment clones that fall into each pattern, shown for all clones in the posttreatment sample as well as clones that could be identified as CD8$^+$ or CD4$^+$ by TCR deep sequencing of purified subsets.

Published OnlineFirst September 24, 2014; DOI: 10.1158/2326-6066.CIR-14-0154

by a relative increase in the frequency of $CD3^+$ T cells in the posttreatment tumor (data not shown). Consistent with the establishment of an activated immune milieu, PD-L2 transcript levels (induced by a proinflammatory state) were elevated after treatment, and CSF1R transcript levels, associated with immunosuppressive M2 macrophage function, were reduced in the posttreatment sample. Evidence for neoangiogenesis could also be observed, with elevations in transcripts for VEGF-A, CD34, and PECAM. Notably, gene expression of 5 melanoma-specific antigens that were highly expressed before treatment was decreased or became undetectable in the posttreatment tumor.

Quantification, characterization, and persistence of the tumor-infiltrating T-cell repertoire

Next-generation deep sequencing of the TCRβ locus was performed on DNA from the pretreatment and posttreatment biopsy samples to understand and quantify the diversity of the tumor-infiltrating T-cell populations. There were 2,096 unique T-cell clones identified in the pretreatment specimen (Fig. 3A, red), and 6,984 unique clones identified in the posttreatment tumor (Fig. 3A, blue). In both pretreatment and posttreatment samples, we identified a skewed distribution of tumor-infiltrating T-cell clones, with a relatively low number of unique clones accounting for the collection of the most frequent clones. In the posttreatment sample, only 652 unique clones were found with a frequency higher than 0.03%, and only 3 unique clones were higher than 1% (Fig. 3A). These skewed clonal populations in each sample are further illustrated by the calculation that the top 2% to 3% of the most frequent unique clones comprised 25% of all T cells in the sample (the TQ; Fig. 3B). In the pretreatment tumor, there were 61 clones in the TQ, comprising 2.8% of all unique clones in the sample, with an average frequency of 0.34% (range, 0.20%–1.30%); in the posttreatment tumor, there were 127 clones in the TQ, comprising 1.8% of all unique clones, with an average frequency of 0.16% (range, 0.06%–1.32%; Fig. 3C).

There was little overlap in the population of unique clones detected in the pretreatment versus posttreatment tumor, indicating a near complete alteration in the tumor-infiltrating T-cell repertoire at the time of relapse. Among all clones, 148 (1.6%) were identified in both samples. This TCR clonal overlap is lower than that seen when comparing multiple biopsy sites within a single metastatic lesion, or metastases versus primary tumor in a single patient (20). Considering that T-cell clonal expansion is a critical indicator of antigen-specific T-cell immune responses (and that the most frequent T-cell clones in melanoma have been shown to be the most enriched for functional antitumor T cells; ref. 21), we focused further analysis on the TQ subset of clones from each sample. Among such clones in each sample, 10 clones (5.6%) were found in both samples (Fig. 3C). Among all TQ clones from each tumor, the majority was found in either the pretreatment or in the posttreatment samples (but not both), 26.4% and 55.1%, respectively (Fig. 3D). The remaining 18.5% of clones were present in both samples (Fig. 3D). Interestingly, certain clones were low frequency (not TQ) in the pretreatment tumor but became TQ clones following treatment (10.7% of all TQ clones fit this pattern); however, only 2.2% of TQ pretreatment decreased to lower levels in posttreatment sample (Fig. 3D). In summary, the majority of TQ clones in the posttreatment sample were either undetected or at low frequency before treatment, and most TQ clones at pretreatment were not detectable in the relapse specimen (Fig. 3D), underscoring the transition from one T-cell repertoire to another after therapy.

Finally, to understand if *de novo* or expanded T-cell clones identified in the tumor after treatment were associated with a systemic immune response, we performed TCRβ deep sequencing of peripheral blood to identify and track tumor-infiltrating T-cell clones in the patient over a multi-year period. Again focusing on TQ clones in the posttreatment sample, five distinct clonal patterns were noted (Fig. 3E) based on the presence or absence of a particular clone in blood at baseline, appearance or not in the blood posttreatment, and increase or decrease in blood comparing pretreatment with posttreatment. We focused on the TQ posttreatment clones found in the tumor that were not identified in the blood at baseline but became increasingly frequent following treatment (pattern 1, $n = 11$ clones). These clones may represent treatment-induced antitumor T cells. Given the sensitivity of the deep-sequencing approach, it was also possible to identify TQ clones that were present in blood at baseline but that either increased (pattern 2, $n = 24$ clones) or decreased (pattern 3, $n = 12$ clones) over the course of treatment. Lastly, we identified TQ posttreatment clones in the tumor that became undetectable after treatment (pattern 4, $n = 3$ clones) or were never observed (pattern 5, $n = 77$ clones) in the blood. The percentage of each type of clonal frequency pattern, further characterized by CD4 versus CD8 phenotype, is shown in Fig. 3F. From this analysis, we calculate that 25.5% of all TQ clones in the tumor after treatment either appeared or increased in the patient's blood over five years (Fig. 3F, left, pattern 1 plus pattern 2). Similarly, 58.5% of $CD8^+$ TQ clones in the tumor posttreatment either appeared or increased in the patient's blood over 5 years (Fig. 3F, middle). For CD4 T cells, this percentage was 33.3% (Fig. 3F, right). We interpret the coordinated appearance and persistence of T-cell clones in the tumor and blood after treatment as being consistent with a durable, systemic immune response relevant to the patient's clinical outcome.

Discussion

We report a comprehensive immunologic evaluation of a patient with metastatic melanoma who has experienced a long-term, ongoing, complete remission after CD40 antibody therapy and single metastasectomy. We observed induction of an immune activation signature in the tumor microenvironment after treatment, reflected by increased tumor-infiltrating T cells, upregulation of an immune activation gene expression signature, and emergence of a *de novo* T-cell repertoire in the tumor—the latter finding based on the emerging technology of TCR deep sequencing. A large fraction of the T-cell clones found to be most abundant in the posttreatment tumor were also identified in the patient's blood (either appearing *de novo* in blood or increasing from baseline) with persistence of some clones for years after completion of therapy. This major clinical

Published OnlineFirst September 24, 2014; DOI: 10.1158/2326-6066.CIR-14-0154

response was achieved without significant toxicity and in the absence of pharmacologic checkpoint inhibitors for CTLA-4 or PD-1. This clinical case emphasizes the potential of CD40 activation as a novel immune therapy for cancer and underscores a larger role that direct immune activators, especially TNFRs such as CD40, may play in the rapidly emerging field of cancer immunotherapy. Our analysis also highlights the potential use—and limitations—of TCR deep sequencing in cancer immunoassessment.

There has been concern about toxicities associated with T-cell stimulatory agents, including approved agents such as IL2 and investigational agents such as CD137 mAb (22). The agonistic CD28 mAb TGN1412 triggered severe cytokine storm in a trial involving healthy volunteers (23). For the patient described here, treatment with the CD40 agonist CP-870,893 was well tolerated except for transient, infusion-related cytokine-release syndrome, which was managed in the outpatient setting. Acute elevations in cytokines in the serum of this patient were more than one log lower than that reported for TGN1412 (12, 23). CP-870,893 has not been associated with delayed autoimmune sequelae such as colitis, thyroiditis, or hypophysitis (2).

Although the patient developed a new FDG-avid mass, which raised a concern about progressive disease after completion of 10 cycles of CD40 mAb treatment, immunologic evaluation of this lesion upon biopsy was consistent with T-cell activation, suggesting a response rather than an overt tumor progression. Evidence of broadly emerging clonal populations of T cells that persisted in the circulation for many years, together with a sustained and complete remission 9 years after treatment, suggests a mechanism for agonistic CD40 immunotherapy involving activation of potent antitumor T-cell immunity and induction of long-lasting T-cell–mediated memory. This interpretation is consistent with findings from preclinical mouse models that had demonstrated the ability of agonist CD40 mAbs to activate APCs and mobilize antitumor T cells (7–9).

The manageable toxicity of agonist CD40 mAbs and their mechanisms of action suggest a potentially favorable combination partner with anti–CTLA-4 mAbs, which promote T-cell activation and diminish the effects of regulatory T cells, and anti–PD-1 or anti–PD-L1 mAbs, which relieve immunosuppressive mechanisms that dampen an already existing $CD8^+$ T-cell response (24, 25). Agonistic CD40 mAbs may enhance APC-mediated activation of $CD8^+$ T cells, broadening the effective $CD8^+$ T-cell repertoire. A combination of CD40 agonists with blockade of negative immune checkpoints may potentially retard immune escape to CTLA-4 or PD-1 blockade alone.

In our analysis of this patient, we explored the use of TCR deep sequencing as an emerging technology to track T-cell immune responses following immunomodulatory cancer therapy (11, 19, 21, 26). We hypothesized that this strategy would provide a repertoire-wide assessment of T-cell responses in both the tumor and blood of a patient with a major clinical response. As with other immunomodulatory agents, such as CTLA-4 or PD-1 mAbs, treatment with CP-870,893 does not explicitly target a particular T-cell epitope that could be tracked in patients with peptide-specific tools such as peptide–MHC tetramers. The biologic significance and the role of TCR deep sequencing, however, are only beginning to be appreciated. The technology provides two types of information: the sequence identity of the TCRβ chains found within the sample and the relative frequency of each of these unique chains. Enumeration of unique TCRβ sequences in a given population allows estimation of the overall diversity of a given T-cell population and identification of high-frequency clones of interest. Changes in diversity may help elucidate the mechanism of action, but these measurements have not yet proven to be predictive or prognostic (19, 26). Here, in the absence of a defined therapeutic T-cell target, we focused (or "gated") our analysis on T-cell clones found in the tumor microenvironment. Although this strategy by no means assures tumor specificity of tumor-infiltrating T-cell clones identified, we hypothesized that tumor-infiltrating clones would be enriched for tumor specificity compared with unfractionated blood. Thus, for our longitudinal assessment of blood T-cell clones from this patient, we "gated" our analysis on only those clones found at least once in the tumor microenvironment, with a particular interest on those tumor clones with highest prevalence. T-cell clonal expansion following antigen recognition and priming suggests, biologically, that T cells with tumor antigen–specific TCR should be present at relatively higher rates in the tumor than their antigen-naïve, nonexpanded, counterparts. However, this expected proliferation of tumor antigen–specific T cells cannot be formally proven with TCRβ deep sequencing alone. Moreover, because we did not sequence the TCRα chain and match it with its corresponding TCRβ chain, we did not identify completely unique T cells with single-antigen specificity. Indeed, TCRβ deep sequencing alone cannot determine the antigen specificity of an immune response, although we have developed an indirect method to assign CD8 versus CD4 phenotype to T-cell clones of interest using data from sorted populations retrospectively applied to archival samples. Other issues with TCR deep sequencing include sampling error from tumor heterogeneity and sensitivity of the assay for extremely rare clones. In summary, we found that TCR deep sequencing applied simultaneously to sequential samples of tumor and blood can reveal new information beyond traditional assay methods, such as tetramers or ELISPOT, and is worthy of further study and application.

Disclosure of Potential Conflicts of Interest

C. Desmarais has ownership interest (including patents) in Adaptive Biotechnologies. M. Kalos is a consultant/advisory board member for Adaptive Biotechnologies. R.H. Vonderheide reports receiving a commercial research grant from Roche and Pfizer. No potential conflicts of interest were disclosed by the other authors.

Authors' Contributions

Conception and design: D.L. Bajor, R. Mick, R.H. Vonderheide

Development of methodology: D.L. Bajor, L.P. Richman, M. Kalos, R.H. Vonderheide

Acquisition of data (provided animals, acquired and managed patients, provided facilities, etc.): D.L. Bajor, X. Xu, L.R. Garcia, K.L. Nathanson, L.M. Schuchter, M. Kalos, R.H. Vonderheide

Analysis and interpretation of data (e.g., statistical analysis, biostatistics, computational analysis): D.L. Bajor, D.A. Torigian, R. Mick, L.P. Richman, C. Desmarais, K.L. Nathanson, M. Kalos, R.H. Vonderheide

Published OnlineFirst September 24, 2014; DOI: 10.1158/2326-6066.CIR-14-0154

Writing, review, and/or revision of the manuscript: D.L. Bajor, X. Xu, D.A. Torigian, R. Mick, C. Desmarais, K.L. Nathanson, L.M. Schuchter, M. Kalos, R.H. Vonderheide
Administrative, technical, or material support (i.e., reporting or organizing data, constructing databases): L.R. Garcia, C. Desmarais, R.H. Vonderheide
Study supervision: R.H. Vonderheide

Acknowledgments

The authors thank James Riley, Carl June, Tara Gangadhar, Matthew Reise, Hank Pletcher, Andrew Wells, Maryanne Gallagher, and Amy Kramer at the University of Pennsylvania for helpful discussions.

Grant Support

This work was supported by NIH grants R01 CA158786 (to R.H. Vonderheide), T32 HL007775-16 (to D.L. Bajor), and P30 CA016520 (to R. Mick, D.A. Torigian, K. L. Nathanson, L.M. Schuchter, and R.H. Vonderheide), the Prostate Cancer Foundation (to D.L. Bajor), and Pfizer Corp (to R.H. Vonderheide).

The costs of publication of this article were defrayed in part by the payment of page charges. This article must therefore be hereby marked *advertisement* in accordance with 18 U.S.C. Section 1734 solely to indicate this fact.

Received August 19, 2014; revised September 11, 2014; accepted September 15, 2014; published OnlineFirst September 24, 2014.

References

1. van Kooten C, Banchereau J. CD40-CD40 ligand. J Leukoc Biol 2000;67:2–17.
2. Vonderheide RH, Glennie MJ. Agonistic CD40 antibodies and cancer therapy. Clin Cancer Res 2013;19:1035–43.
3. Lougaris V, Badolato R, Ferrari S, Plebani A. Hyper immunoglobulin M syndrome due to CD40 deficiency: clinical, molecular, and immunological features. Immunol Rev 2005;203:48–66.
4. Heath WR, Bennett SRM, Carbone FR, Karamalis F, Flavell RA, Miller JFAP. Help for cytotoxic-T-cell responses is mediated by CD40 signalling. Nature 1998;393:478–80.
5. Schoenberger SP, Toes REM, van der Voort EIH, Offringa R, Melief CJM. T-cell help for cytotoxic T lymphocytes is mediated by CD40-CD40L interactions. Nature 1998;393:480–3.
6. Ridge JP, Di Rosa F, Matzinger P. A conditioned dendritic cell can be a temporal bridge between a CD4+ T-helper and a T-killer cell. Nature 1998;393:474–8.
7. French RR, Chan HTC, Tutt AL, Glennie MJ. CD40 antibody evokes a cytotoxic T-cell response that eradicates lymphoma and bypasses T-cell help. Nat Med 1999;5:548–53.
8. Diehl L, Boer den AT, Schoenberger SP, van der Voort EIH, Schumacher TNM, Melief CJM, et al. CD40 activation in vivo overcomes peptide-induced peripheral cytotoxic T-lymphocyte tolerance and augments anti-tumor vaccine efficacy. Nat Med 1999;5:774–9.
9. Sotomayor EM, Borrello I, Tubb E, Rattis F-M, Bien H, Lu Z, et al. Conversion of tumor-specific CD4 +T-cell tolerance to T-cell priming through in vivo ligation of CD40. Nat Med 1999;5:780–7.
10. Gladue RP, Paradis T, Cole SH, Donovan C, Nelson R, Alpert R, et al. The CD40 agonist antibody CP-870,893 enhances dendritic cell and B-cell activity and promotes anti-tumor efficacy in SCID-hu mice. Cancer Immunol Immunother 2011;60:1009–17.
11. Richman LP, Vonderheide RH. Role of crosslinking for agonistic CD40 monoclonal antibodies as immune therapy of cancer. Cancer Immunol Res 2014;2:19–26.
12. Vonderheide RH, Flaherty KT, Khalil M, Stumacher MS, Bajor DL, Hutnick NA, et al. Clinical activity and immune modulation in cancer patients treated with CP-870,893, a novel CD40 agonist monoclonal antibody. J Clin Oncol 2007;25:876–83.
13. Rüter J, Antonia SJ, Burris HA, Huhn RD, Vonderheide RH. Immune modulation with weekly dosing of an agonist CD40 antibody in a phase I study of patients with advanced solid tumors. Cancer Biol Ther 2010;10:983–93.
14. Beatty GL, Chiorean EG, Fishman MP, Saboury B, Teitelbaum UR, Sun W, et al. CD40 agonists alter tumor stroma and show efficacy against pancreatic carcinoma in mice and humans. Science 2011;331:1612–6.
15. Beatty GL, Torigian DA, Chiorean EG, Saboury B, Brothers A, Alavi A, et al. A phase I study of an agonist CD40 monoclonal antibody (CP-870,893) in combination with gemcitabine in patients with advanced pancreatic ductal adenocarcinoma. Clin Cancer Res 2013;19:6286–95.
16. Vonderheide RH, Burg JM, Mick R, Trosko JA, Li D, Shaik MN, et al. Phase I study of the CD40 agonist antibody CP-870,893 combined with carboplatin and paclitaxel in patients with advanced solid tumors. Oncoimmunology 2013;2:e23033.
17. Yun SJ, Gimotty PA, Hwang W-T, Dawson P, Van Belle P, Elder DE, et al. High lymphatic vessel density and lymphatic invasion underlie the adverse prognostic effect of radial growth phase regression in melanoma. Am J Surg Pathol 2011;35:235–42.
18. Robins H, Desmarais C, Matthis J, Livingston R, Andriesen J, Reijonen H, et al. Ultra-sensitive detection of rare T cell clones. J Immunol Methods 2012;375:14–9.
19. Cha E, Klinger M, Hou Y, Cummings C, Ribas A, Faham M, Fong L. Improved survival with T cell clonotype stability after anti-CTLA-4 treatment in cancer patients. Sci Transl Med 2014;6:238ra70.
20. Emerson RO, Sherwood AM, Rieder MJ, Guenthoer J, Williamson DW, Carlson CS, et al. High-throughput sequencing of T cell receptors reveals a homogeneous repertoire of tumor-infiltrating lymphocytes in ovarian cancer. J Pathol 2013;231:433–40.
21. Gros A, Robbins PF, Yao X, Li YF, Turcotte S, Tran E, et al. PD-1 identifies the patient-specific CD8+ tumor-reactive repertoire infiltrating human tumors. J Clin Invest 2014;124:2246–59.
22. Gangadhar TC, Vonderheide RH. Mitigating the toxic effects of anticancer immunotherapy. Nat Rev Clin Oncol 2014;11:91–9.
23. Suntharalingam G, Perry MR, Ward S, Brett SJ, Castello-Cortes A, Brunner MD, et al. Cytokine storm in a phase 1 trial of the anti-CD28 monoclonal antibody TGN1412. N Engl J Med 2006;355:1018–28.
24. Hamid O, Robert C, Daud A, Hodi FS, Hwu W-J, Kefford R, et al. Safety and tumor responses with lambrolizumab (Anti–PD-1) in melanoma. N Engl J Med 2013;369:134–44.
25. Wolchok JD, Kluger H, Callahan MK, Postow MA, Rizvi NA, Lesokhin AM, et al. Nivolumab plus Ipilimumab in advanced melanoma. N Engl J Med 2013;369:122–33.
26. Robert L, Tsoi J, Wang X, Emerson RO, Homet B, Chodon T, et al. CTLA4 blockade broadens the peripheral T cell receptor repertoire. Clin Cancer Res 2014;20:2424–32.

Published OnlineFirst September 24, 2014; DOI: 10.1158/2326-6066.CIR-14-0154

Cancer Immunology Research

Immune Activation and a 9-Year Ongoing Complete Remission Following CD40 Antibody Therapy and Metastasectomy in a Patient with Metastatic Melanoma

David L. Bajor, Xiaowei Xu, Drew A. Torigian, et al.

Cancer Immunol Res 2014;2:1051-1058. Published OnlineFirst September 24, 2014.